Bioactive Ginger Constituents Alleviate Protein Glycation by Trapping Methylglyoxal

ARTICLE *in* CHEMICAL RESEARCH IN TOXICOLOGY · AUGUST 2015

Impact Factor: 3.53 · DOI: 10.1021/acs.chemrestox.5b00293 · Source: PubMed

5 AUTHORS, INCLUDING:

Yingdong Zhu

North Carolina Agricultural and Technical Stat…

30 PUBLICATIONS **251** CITATIONS

SEE PROFILE

Yantao Zhao

North Carolina Agricultural and Technical Stat…

21 PUBLICATIONS **129** CITATIONS

SEE PROFILE

Pei Wang

North Carolina Agricultural and Technical Stat…

23 PUBLICATIONS **72** CITATIONS

SEE PROFILE

Mohamed Ahmedna

Qatar University

62 PUBLICATIONS **2,194** CITATIONS

SEE PROFILE

Chemical Research in Toxicology

Article

pubs.acs.org/crt

Bioactive Ginger Constituents Alleviate Protein Glycation by Trapping Methylglyoxal

Yingdong Zhu,[†] Yantao Zhao,[†] Pei Wang,[†] Mohamed Ahmedna,[‡] and Shengmin Sang*[,†]

[†]Center for Excellence in Post-Harvest Technologies, North Carolina Agricultural and Technical State University, North Carolina Research Campus, 500 Laureate Way, Kannapolis, North Carolina 28081, United States

[‡]Department of Health Science, College of Arts & Sciences, Qatar University, Doha 2713, Qatar

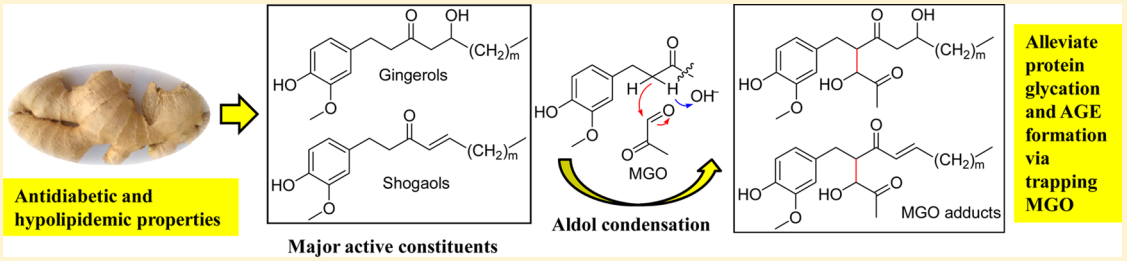

ABSTRACT: Considerable evidence suggests that long-term pathological diabetes is a result of the accumulation of tissue macromolecules that have been progressively modified by nonenzymatic glycation of protein. Methylglyoxal (MGO) is a highly reactive endogenous dicarbonyl metabolite derived from multiple sources such as glucose and lipids and is thought to contribute greatly to protein glycation and the formation of advanced glycation end products (AGEs). In this study, we demonstrated for the first time that both [6]-shogaol (6S) and [6]-gingerol (6G), the major active components in ginger, markedly trapped MGO *in vitro* and consequently formed mono-MGO adducts, 6S-MGO and 6G-MGO, which were purified from the respective chemical reaction and characterized as novel compounds by NMR experiments and LC−MS/MS approaches. We revealed that the α-carbon of the carbonyl group in the side chain of 6S or 6G is the major active site for trapping MGO. We also demonstrated that 6S and 6G could effectively inhibit the formation of MGO-induced AGEs via trapping MGO in a time-dependent manner in the human serum albumin (HSA)−MGO system. Mono-MGO adducts, 6S-MGO and 6G-MGO, were determined to be the major conjugates in 6S- and 6G-treated HSA−MGO assays, respectively, using LC−ESI-MS techniques. These findings showed the potential effects of 6S and 6G on the prevention of protein glycation, suggesting regular consumption of ginger root extract may attenuate the progression of MGO-associated diabetic complications in patients.

INTRODUCTION

Diabetes mellitus is a group of disorders that result from insulin deficiency and/or insulin resistance. Both insulin deficiency and insulin resistance in diabetes produce an abnormal increase in blood glucose, resulting in hyperglycemia. Prolonged hyperglycemia and glucose metabolic disorders associated with diabetes mellitus produce a large number of reactive carbonyl compounds, such as methylglyoxal (MGO), glyoxal (GO), and 3-deoxyglucosone, and other saccharide derivatives.[1] Carbonyl compounds such as MGO may play an important role in the development of insulin resistance.[2] Glycation of proteins is implicated in a number of biochemical abnormalities associated with aging and diabetes. Glycation involves the nonenzymatic addition of reducing sugars and/or their degradation products, such as MGO and GO, to primary or secondary amine groups of arginine and lysine residues on proteins,[1] which alters protein conformation and stability and induces protein aggregation and cross-linking,[3,4] eventually resulting in the formation of irreversible advanced glycation end products (AGEs).[5−7] Although the formation of AGEs takes place during the aging process, it is accelerated under hyperglycemic conditions. Accumulation of AGEs in various tissues has been known to be related to the severity of chronic diabetic complications such as nephropathy, neuropathy, retinopathy, and cataract,[7,8] as well as to cause Parkinson's disease,[9] Alzheimer's disease,[10] and aging.[11] Therefore, compounds with the capacity to reduce cellular and peripheral free dicarbonyl species by either trapping or detoxification are expected to inhibit the formation of AGEs and may prevent the progression of diabetic complications.

MGO, the most reactive AGE precursor, is a major reactive dicarbonyl species in the human body. It was reported that plasma levels of MGO are significantly lower in healthy volunteers (0.4−1.0 μM) than in diabetic patients (2.2−3.8 μM).[12] Fluorescent and cross-linking AGEs, such as 1,3-di-N^{ε}-lysino-4-methylimidazolium,[13] and nonfluorescent/non-cross-linking AGEs, including N^{ε}-(carboxymethyl)lysine (CML), can be readily formed and accumulate because of the reactive free MGO.[14] Hyperglycemia-induced formation of AGEs is considered the main cause of diabetes-related complications.[15] Therapeutic strategies to prevent or alleviate diabetic

Received: July 13, 2015
Published: August 6, 2015

DOI: 10.1021/acs.chemrestox.5b00293
Chem. Res. Toxicol. 2015, 28, 1842−1849

complications are to use either antihyperglycemic agents or AGE inhibitors. Several types of drugs such as sulfonylurea and thiazolidinedione are prescribed for treating hyperglycemia in type 2 diabetic patients.[16] Many anti-AGE agents, such as aminoguanidine,[17] carnosine,[18] and tenilsetam,[19] have been investigated as inhibitors of the formation of AGEs and the development of diabetic complications by trapping dicarbonyl species. However, each drug or inhibitor has adverse side effects,[20,21] so there is great interest in developing natural interventions combining higher levels of selectivity and safety for managing diabetes and its symptoms.

Ginger (*Zingiber officinale*) is one of the most widely consumed spices worldwide and has been used as an herbal medicine to treat a variety of ailments, including vomiting, pain, indigestion, and cold-induced syndromes, in the traditional medicinal system of Asia for centuries.[22] Ginger is generally considered safe. Clinical trials demonstrated that pregnant women consuming 1.0−1.5 g of ginger extract daily for ease of nausea and vomiting suffered no obvious safety issues, major malformations, or other birth defects compared to the general population.[23,24] A 35-day toxicity study indicated that oral administration of ginger powder up to 2 g/kg once daily did not cause any mortality or abnormal changes in the general condition or hematological parameters in either male or female rats.[25] Recently, researchers have realized that, in addition to anticancer, anticlotting, and antiinflammatory activities,[26,27] ginger has the potency to treat diabetes mellitus and diabetic complications in liver, kidney, eyes, and the central nervous system.[28,29] For instance, an animal study discovered that a diet containing 0.5 or 3% freeze-dried ginger powder significantly inhibited the formation of various AGEs and countered hyperglycemia-induced osmotic stress in the lens of rats, therefore effectively delaying the development of diabetic cataract in rats.[30] Furthermore, a recent human study has shown that intake of 2 g of ginger powder supplement per day for 12 weeks significantly reduced the levels of fasting blood sugar and hemoglobin A1c in type 2 diabetic patients.[31] Another double-blind clinical trial demonstrated that daily consumption of three 1 g capsules of ginger powder for 8 weeks could also reduce hemoglobin A1c levels in patients with type 2 diabetes.[32] However, little is known about the mechanisms underlying the prevention of diabetes and related complications by ginger extract or ginger components. The most active ingredients in ginger are the pungent principles, gingerols, and shogaols.[33] [6]-Gingerol (6G) is the most abundant pungent constituent in fresh roots of ginger, while [6]-shogaol (6S) is the most abundant one in dried and thermally treated roots.[34] In this study, we measured the MGO trapping capability of 6S and 6G under simulated physiological conditions, and in particular, we investigated the formation of MGO adducts of 6S and 6G generated from the chemical reaction between MGO and 6S/6G using NMR experiments and LC−MS/MS techniques. We also tested the potency of 6S and 6G for inhibiting the formation of AGEs by trapping MGO in the HSA−MGO system and proposed an underlying mechanism for the inhibition, as well.

MATERIALS AND METHODS

Materials. 6S and 6G were purified from ginger root extract in our laboratory.[35] MGO (40% in water), 1,2-diaminobenzene (OPD), and 2-methylquinoxaline were purchased from Sigma (St. Louis, MO). HPLC-grade solvents and other reagents were obtained from Thermo Fisher Scientific (Waltham, MA). Analytical (250 μm thickness, 2−25 μm particle size) and preparative TLC plates (1000 μm thickness, 2−25 μm particle size) were purchased from Sigma and Sorbent Technologies (Atlanta, GA), respectively. Human serum albumin (HSA) was obtained from Sigma.

Kinetic Study of the Trapping of MGO by 6S and 6G. MGO (0.33 mM) was incubated with 1.0 mM 6S or 6G in a phosphate buffer solution (PBS) (160 μL, pH 7.4, 100 mM). The mixed solutions were incubated at 37 °C and shaken at 40 rpm for 0, 10, 30, 60, and 360 min. Next, to each triplicate vial at each time point was added 1 μL of acetic acid (AA) to stop the reaction followed by an additional 40 μL of 100 mM 1,2-diaminobenzene (OPD) in PBS. The mixture was further incubated in the dark at 37 °C for 30 min. The resulting solution was diluted 10-fold, and 80 μL was analyzed via HPLC. The level of 2-methylquinoxaline formed was used to reflect the contents of the remaining MGO (percent) in PBS (Figure 1A). The recovery of 2-methylquinoxaline was more than 95% (data not shown).

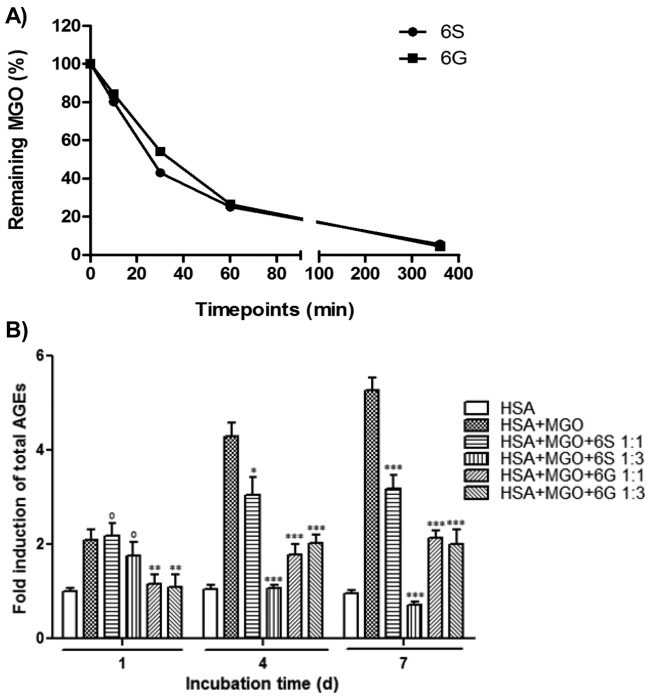

Figure 1. Trapping of MGO and inhibition of MGO-induced formation of AGEs by 6S and 6G. (A) Kinetic curves for trapping of MGO by 6S and 6G in PBS (pH 7.4, 37 °C). MGO (0.33 mM) was incubated with 1.0 mM 6S or 6G in PBS (pH 7.4, 37 °C) for 0, 10, 30, 60, and 360 min. Results are means ± SD (n = 3). (B) Inhibitory effect of 6S or 6G on MGO-induced formation of AGEs in a HSA−MGO assay. HSA (1.4 mg/mL) was incubated with MGO (0.5 mM) in the presence or absence of 6S or 6G (0.5 and 1.5 mM) in PBS (pH 7.4, 37 °C) for 1, 4, and 7 days. HSA was used as a negative control. HSA +MGO was used as a positive control. Results are means ± SD (n = 4). Symbol: bar, standard deviation; o, not significant; *p < 0.05; **p < 0.001; ***p < 0.0001. All statistical tests are unpaired Student's t tests, two-tailed, compared to the positive control.

HPLC Analysis. The level of 2-methylquinoxaline was analyzed using an HPLC system, consisting of an ESA model 584 HPLC pump, an ESA model 542 autosampler, an ESA organizer, and an ESA 526 UV detector. A Gemini C_{18} column [150 mm × 4.6 mm, 5 μm (Phenomenex, Torrance, CA)] was used for chromatographic analysis at a flow rate of 1.0 mL/min. HPLC was performed under binary gradient elution as described in our previous study with some modifications.[36] In short, the column was eluted with a binary gradient system: 100 to 75% A from 0 to 5 min, 75 to 65% A from 5 to 15 min, 65 to 0% A from 15 to 18 min, 0% A from 18 to 23 min, and then 100% A from 23 to 28 min. The injection volume was 10 μL. The

DOI: 10.1021/acs.chemrestox.5b00293
Chem. Res. Toxicol. 2015, 28, 1842−1849

wavelength of the UV detector was set at 280 nm with 100 ng/mL as the limit of detection and 1 μg/mL as the limit of quantification for 2-methylquinoxaline.

Inhibitory Effects of 6S and 6G on the Formation of AGEs in the HSA−MGO System. HSA (1.4 mg/mL) was incubated with MGO (0.5 mM) in the presence or absence of 6S or 6G (0.5 and 1.5 mM) in PBS (pH 7.4, 100 mM) at 37 °C for 1, 4, and 7 days. A mixed solution of streptomycin and penicillin was added before incubation to prevent bacterial growth. The AGE levels of the reacted mixtures harvested on days 1, 4, and 7 were quantified using fluorescence at 360 nm excitation and 460 nm emission wavelengths by a multimode microplate reader (Synergy 2, Biotek). The fluorescence intensity was expressed in arbitrary units (AU), and the fluorescence was normalized to that of HSA incubated without MGO.

Synthesis and Purification of the Major MGO Adducts of 6S and 6G. To a solution of 6S (138 mg, 0.5 mmol, 1.0 equiv) in a mixture of PBS and methanol [3 mL; 1:2 (v/v)] was added a 40% MGO aqueous solution (270 μL, 1.5 mmol, 3.0 equiv) followed by 4 drops of a saturated $NaHCO_3$ solution. The mixture was incubated at 37 °C for 8 h, acidified with a 20% HCl solution, and extracted with ethyl acetate (EA) (3 × 5 mL). The organic solvent was removed *in vacuo*. The residue was purified by repeated preparative TLC (2:1 hexane/EA) to give 6S-MGO (15 mg) as a yellow oil. Likewise, 6G (147 mg, 0.5 mmol, 1.0 equiv) was reacted with 40% MGO (270 μL, 1.5 mmol, 3.0 equiv) under the condition described above. The residue was purified by repeated preparative TLC (20:1 $CHCl_3$/MeOH) to give 6G-MGO (8 mg) as a yellow oil.

NMR Analysis. ^1H, ^{13}C, and two-dimensional (2D) NMR spectra were recorded on a Bruker AVANCE 600 MHz spectrometer (Bruker, Silberstreifen, Rheinstetten, Germany). 6S-MGO and 6G-MGO were analyzed in $CDCl_3$, with TMS as an internal standard. Multiplicities are indicated by s (singlet), d (doublet), t (triplet), q (quartet), and br (broad). The ^{13}C NMR spectra are proton-decoupled.

Investigation of the Formation of MGO Adducts of 6S and 6G under Simulated Physiological Conditions. MGO (1 mM) and 6S or 6G (0.33 and 3 mM) were dissolved in PBS (162.5 μL, pH 7.4, 100 mM). The mixed solutions were incubated at 37 °C and shaken at 150 rpm for 1 and 24 h. To each vial at each time point was added 5 μL of AA to stop the reactions. The resulting solution was diluted 1000-fold and centrifuged at 17000*g* for 10 min, and 50 μL of the supernatant was analyzed by LC−MS. 6S-MGO and 6G-MGO in methanol (1 μM for each) were used as authentic references.

LC−MS Analysis. LC−MS analysis was conducted with a Thermo-Finnigan Spectra System that consists of a Dionex XRS pump, a Dionex XRS open autosampler, and a LTQ Velos Pro ion trap mass detector (Thermo Electron, San Jose, CA) incorporated with an electrospray ionization (ESI) interface. A Gemini C_{18} column (150 mm × 4.6 mm inside diameter, 5 μm, Phenomenex) was used to analyze MGO adducts with a flow rate of 0.3 mL/min. The binary mobile phase system consists of 5% aqueous methanol with 0.1% formic acid (FA) as phase A and methanol with 0.1% FA as phase B. The column was eluted with a gradient progress (30% B from 0 to 2 min, 30 to 85% B from 2 to 7 min, 85 to 100% B from 7 to 13 min, 100% B from 13 to 23 min, and then 30% B from 23 to 25 min). The injection volume was 20 μL for each sample. The LC eluate was introduced into the ESI interface. The positive ion polarity mode was set for an ESI ion source with the voltage on the ESI interface maintained at approximately 3.6 kV. Nitrogen gas was used as the sheath gas at a flow rate of 34 AU and the auxiliary gas at 10 AU. The collision-induced dissociation was conducted with an isolation width of 1.0 Da and a normalized collision energy of 35 for MS/MS analysis. The mass range was measured from *m/z* 50 to 500. Data were acquired with Xcalibur version 2.0 (Thermo Electron).

Determining the Formation of MGO Adducts of 6S and 6G in the HSA−MGO System via LC−MS. HSA (1.4 mg/mL) was incubated with MGO (0.5 mM) in the presence of 6S or 6G (0.5 mM) in PBS (pH 7.4, 100 mM) at 37 °C for 1, 4, and 7 days. To each medium (100 μL) harvested on days 1, 4, and 7 was added 900 μL of methanol. The mixture was vortexed vigorously. The suspension was diluted 100-fold and centrifuged at 17000*g* for 10 min. The supernatant (50 μL) was transferred into vials and analyzed by LC−MS utilizing the method described above.

Statistical Analysis. Statistical analysis was conducted using GraphPad Prism (version 5). For simple comparisons between two groups, a two-tailed Student's *t* test was used. A *p* value of <0.05 was considered to be statistically significant in all tests.

RESULTS

Kinetic Study of the Trapping of MGO by 6S and 6G. The trapping abilities of 6S and 6G were evaluated in PBS (pH 7.4, 100 mM) at 37 °C. The kinetic curves of the trapping of MGO by 6S or 6G during the course of 360 min show that MGO in PBS was captured by both compounds, with each exerting a comparable scavenging ability (Figure 1A). Approximately 80% of MGO in treated mixtures was scavenged after incubation for 60 min, and <5% of MGO remained after incubation for 360 min. These observations demonstrated that both 6S and 6G could effectively trap MGO *in vitro*.

Inhibitory Effects of 6S and 6G on the Formation of AGEs in the HSA−MGO System. As shown in Figure 1B, except for the 6S-treated groups (1:1 and 1:3 MGO:6S) harvested after incubation for 1 day ($p > 0.10$ for both), all assays showed significant inhibitory effects on the formation of MGO-induced AGEs, compared to the positive control, HSA +MGO ($p < 0.05$ for all).

Purification and Structural Elucidation of the Major MGO Adducts of 6S and 6G. Two MGO adducts, 6S-MGO and 6G-MGO, were carefully purified from the reaction between 6S and 6G and MGO (1:3 6S:MGO or 6G:MGO), respectively (Figure 2). Their structures were characterized by

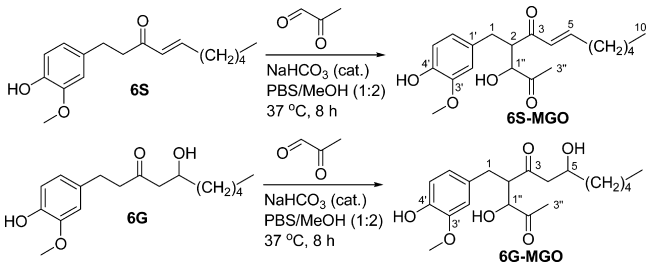

Figure 2. Synthesis of the mono-MGO adducts of 6S and 6G, 6S-MGO and 6G-MGO, respectively.

analyzing their ^1H, ^{13}C, and 2D NMR (DEPT, HSQC, $^1H-^1H$ COSY, and HMBC) spectra as well as their tandem MS spectra (Table 1 and Figure 3). In detail, 6S-MGO, synthesized from 6S and MGO, had a molecular formula of $C_{20}H_{28}O_5$ based on its positive ESI-MS at *m/z* 349 $[M + H]^+$ (276 + 72) and its NMR data. The molecular weight of 6S-MGO was 72 mass units higher than that of 6S,[35] indicating that 6S-MGO is the MGO conjugate of 6S. The appearance of a characteristic acetyl group (δ_H 2.16 and δ_C 26.7 for the methyl group and δ_C 209.4 for the carbonyl group) and an oxygenated methine (δ_H 4.32 and δ_C 77.0) in the ^1H and ^{13}C NMR spectra of 6S-MGO further confirmed the presence of a MGO residue in this compound. HMBC correlations between H-1 (δ_H 2.73 and δ_H 2.98) and C-1″ (δ_C 77.0), H-2 (δ_H 3.50) and C-2″ (δ_C 209.4), and H-1″ (δ_H 4.32) and C-3 (δ_C 201.9) established the linkage of the MGO residue and 6S moiety between C-2 and C-1″ (Figure 3A). This is also supported by the fragments at *m/z* 273 (corresponding to the loss of a MGO unit) and *m/z* 291 (formed by an allylic cleavage of the C_6-C_7 bond) in the MS/MS spectra of 6S-MGO (Figure 3B). These spectral features

DOI: 10.1021/acs.chemrestox.5b00293
Chem. Res. Toxicol. 2015, 28, 1842−1849

Table 1. δ_H (600 MHz) and δ_C (150 MHz) NMR Spectral Data of MGO Adducts of 6S and 6G ($CDCl_3$, δ in parts per million)

	6S-MGO		6G-MGO	
	δ_H	δ_C	δ_H	δ_C
1	2.98 dd, 14.0, 9.0 2.73 dd, 14.0, 5.8	32.8 t	3.16 dd, 14.3, 6.8 2.64 d, 14.3	33.8 t
2	3.50 m	53.8 d	2.58 m	56.8 d
3		201.9 s		206.8 s
4	6.03 d, 15.7	129.3 d	2.70 m 2.60 m	36.9 t
5	6.74 m	150.3 d	3.66 m	70.0 d
6	2.10 m	32.6 t	1.47 m	25.1 t
7	1.31 m	27.6 t	1.30−1.25 m	27.5 t
8	1.29 m	31.3 t	1.30−1.25 m	31.5 t
9	1.29 m	22.5 t	1.30−1.25 m	22.6 t
10	0.86 t, 7.0	13.9 q	0.88 t, 6.9	14.0 q
1′		130.3 s		130.4 s
2′	6.59 brs	111.9 d	6.72 brs	111.0 d
3′		146.4 s		146.6 s
4′		144.3 s		144.2 s
5′	6.80 d, 8.0	114.3 d	6.83 m	114.3 d
6′	6.61 d, 7.2	121.8 d	6.64 m	120.5 d
OMe-3′	3.81 s	55.9 q	3.81 s	55.9 q
1″	4.32 d, 3.2	77.0 d	4.37 brs	76.1 d
2″		209.4 s		206.8 s
3″	2.16 s	26.7 q	2.01 s	13.3 q

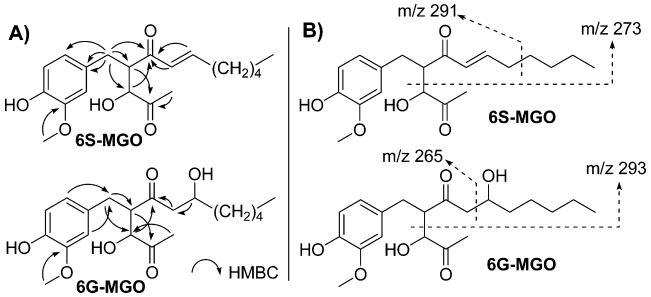

Figure 3. (A) Main HMBC correlations (↷) and (B) characteristic MS/MS fragments of mono-MGO adducts, 6S-MGO and 6G-MGO.

led to the identification of 2-methylglyoxal [6]-shogaol, namely 6S-MGO, which is a novel compound. Likewise, 6G-MGO has a molecular formula of $C_{20}H_{30}O_6$ according to positive ESI-MS at m/z 367 $[M + H]^+$ (294 + 72) and its NMR data and was indicated as the MGO conjugate of 6G. Key HMBC correlations between H-1 (δ_H 2.64 and δ_H 3.16) and C-1″ (δ_C 76.1), H-2 (δ_H 2.58) and C-2″ (δ_C 206.8), and H-1″ (δ_H 4.37) and C-3 (δ_C 206.8) constructed the connection of the MGO residue and 6G moiety between C-2 and C-1″ (Figure 3A). This result was further confirmed by its MS/MS fragments at m/z 265 (formed by α-cleavage of a carbonyl group between C_4 and C_5) and at m/z 293 (corresponding to the loss of a MGO unit) (Figure 3B). Thus, 6G-MGO was identified as 2-methylglyoxal [6]-gingerol, which is a new compound.

Studying the Formation of the MGO Adducts of 6S and 6G under Simulated Physiological Conditions by LC−MS. The reaction mixture of MGO with 6S or 6G at two different ratios (3:1 and 1:3) was collected after incubation for 1 h, and the MGO adducts formed in the reaction mixtures were investigated using LC−MS/MS analysis in selective ion monitoring (SIM) mode. As indicated in Figure 4A, a major peak (t_R = 10.2 min) appeared in the LC chromatograms of 6S-treated medium for both ratios. This peak had a t_R and a MS/MS spectrum almost identical to those of the authentic 6S-MGO that we synthesized and purified from the reaction between 6S and MGO (Figure 4A), demonstrating the formation of 6S-MGO in 6S-treated mixtures under simulated physiological conditions. Moreover, the levels of 6S-MGO formed were proportional to the original compositions of 6S and MGO in the 6S-treated mixtures (Figure 4A). Likewise, 6G-MGO was identified as the major mono-MGO adduct in the 6G-treated mixtures for both ratios (Figures 4B).

Determining the Formation of MGO Adducts of 6S and 6G in the HSA−MGO System Using LC−MS. To improve our understanding of whether the inhibition of AGE formation was caused via the trapping of MGO by 6S and 6G, we determined the existence of the mono-MGO adducts in the treated medium collected at different time points (1, 4, and 7 days) after incubation of the respective 6S and 6G with HSA and MGO (1:1 MGO:6S or MGO:6G) using LC−MS approaches (Figure 5). As a result, a peak with a t_R of 10.2 min appeared in all assays (Figure 5A). This peak had a retention time (Figure 5A) and MS/MS spectra (data not shown) almost identical to those of the authentic 6S-MGO, confirming the formation of the mono-MGO adduct of 6S, 6S-MGO, in the HSA−MGO system. As expected, the level of 6S-MGO increased with time while the level of 6S decreased in the system with time (Figure 5A), indicating that 6S-MGO formed in the system in a time-dependent manner. Similarly, 6G-MGO was determined as the major mono-MGO adduct of 6G in all the 6G-treated assays (Figure 5B).

DISCUSSION

Human serum albumin (HSA) is the most abundant protein in human plasma or serum and is normally present at concentrations ranging from 30 to 50 g/L.[37] HSA is a polypeptide consisting of 585 residues, with 24 arginine residues, 59 lysine residues, and an N-terminus that can act as potential sites for the formation of early stage glycation products and AGEs.[37−39] It has been reported that the level of glycated albumin in diabetic patients is 2−3-fold higher than in a healthy individual.[40] HSA-imposed glycation has been proposed as a tool not only for diagnosing diabetes but also for its potential in assessing diabetes-associated complications.[41] The reactive dicarbonyl species, such as MGO and GO, in humans may account for the formation of HSA-related AGEs, according to the literature about the glycation of HSA by MGO *in vitro*.[42] Therefore, inhibiting glycation of HSA by trapping MGO may prevent or alleviate the development of the related diabetic complications in diabetic patients.

In this study, we reveal for the first time that both 6S and 6G, the major active components of ginger, markedly trap MGO in PBS (pH 7.4, 37 °C) (Figure 1A) and inhibit the formation of MGO-induced AGEs in the HSA−MGO system (Figure 1B). To gain deeper insights into the plausible mechanism of actions underlying the trapping of MGO by 6S and 6G, we investigated the formation of MGO adducts of 6S and 6G by treating MGO with 6S and 6G, respectively. We found evidence of the formation of MGO adducts from both treatments under slightly basic condition after incubation for 8 h (Figure 2). Two mono-MGO adducts, 6S-MGO and 6G-MGO, were purified and identified from the corresponding reaction mixture (Figure 3). Unlike the MGO conjugates of dietary flavonoids in our

DOI: 10.1021/acs.chemrestox.5b00293
Chem. Res. Toxicol. 2015, 28, 1842−1849

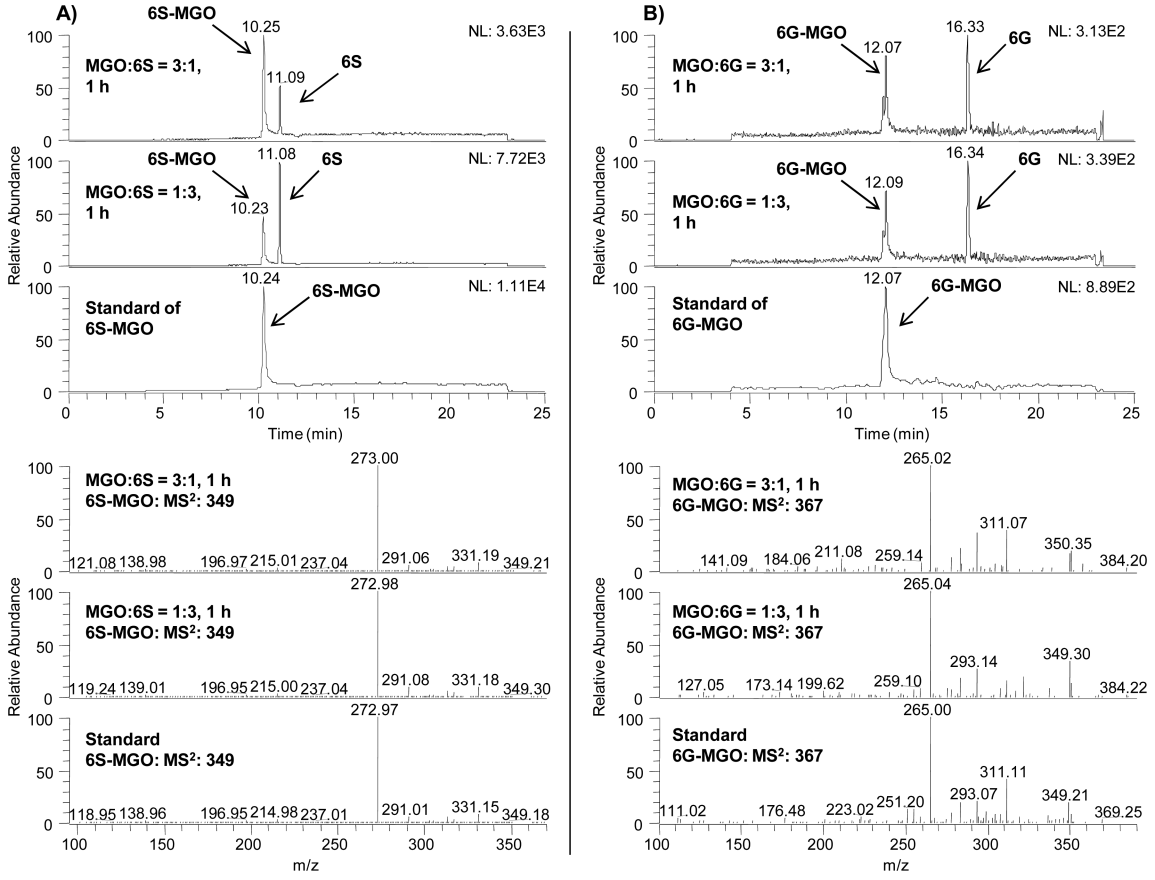

Figure 4. LC chromatograms (SIM) and MS/MS spectra of mono-MGO adducts, (A) 6S-MGO and (B) 6G-MGO, in the 6S- or 6G-treated samples after incubation with MGO (3:1 and 1:3 MGO:6S or MGO:6G) at 37 °C for 1 h as well as corresponding authentic standards obtained by a positive ESI-MS interface. SIM denotes selected ion monitoring and ESI electrospray ionization.

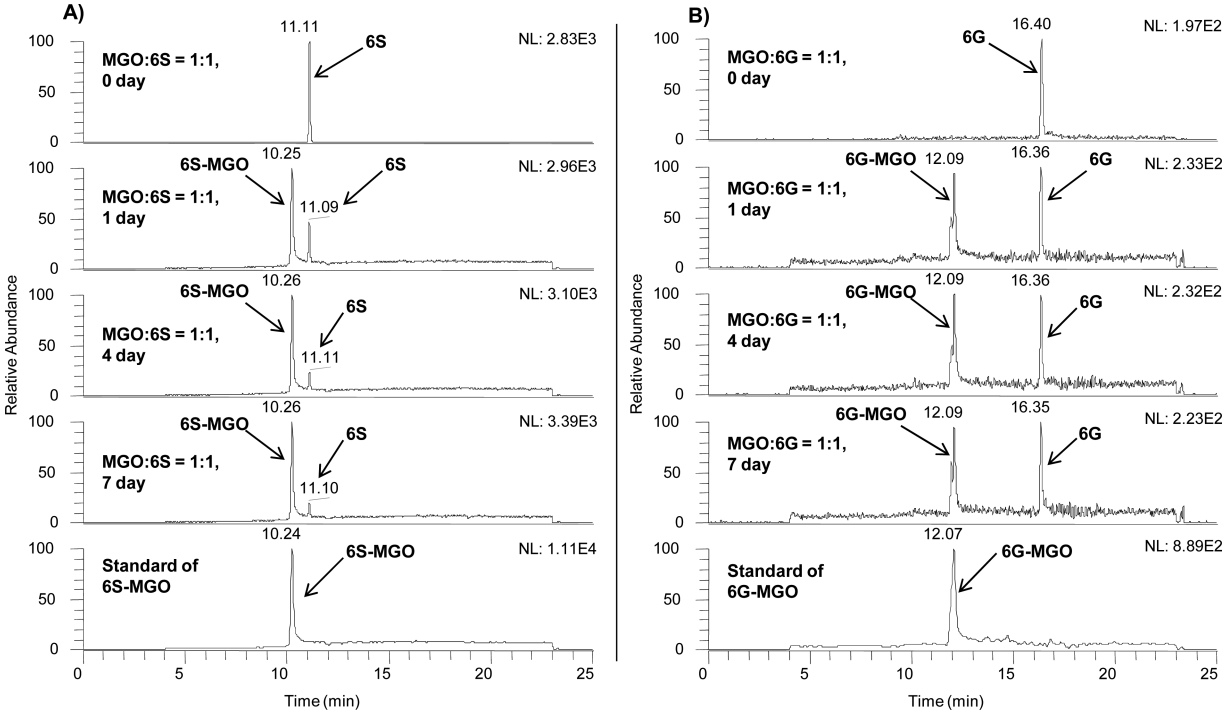

Figure 5. LC chromatograms (SIM) of mono-MGO adducts, (A) 6S-MGO and (B) 6G-MGO, in the 6S- or 6G-treated samples after incubation with HSA and MGO (1:1 MGO:6S or MGO:6G) at 37 °C for 1, 4, and 7 days, as well as corresponding authentic standards obtained by a positive ESI-MS interface.

DOI: 10.1021/acs.chemrestox.5b00293
Chem. Res. Toxicol. 2015, 28, 1842−1849

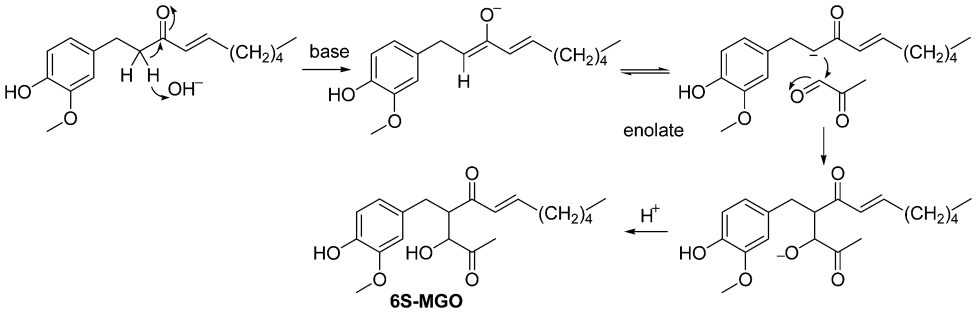

Figure 6. Pathway of formation of the mono-MGO adduct of 6S, 6S-MGO, under simulated physiological conditions.

previous studies, in which the A-ring is the active site of flavonoids,[36,43] we disclosed that MGO was mainly attached to the α-carbon position of the carbonyl group in the side chain of 6S or 6G in this study (Figure 2). In addition, we also found that mono-MGO adducts were predominantly present in either 6S- or 6G-treated medium while the di-MGO adducts were not present under the same conditions. Our results suggested that both 6S and 6G scavenge MGO *in vitro* mainly through the formation of mono-MGO adducts, 6S-MGO and 6G-MGO. Similar to that of curcumin,[44] the chemical pathway for the formation of MGO adducts of 6S or 6G is considered to undergo a classic Aldol condensation because of the active protons of the α-carbonyl group in their structures, as exemplified by 6S in Figure 6. Briefly, deprotonation of the α-carbon of the carbonyl group in 6S by a weak base gives rise to the corresponding enolate as a reactive nucleophile, which subsequently attacks the aldehyde group of MGO in the system to produce the target molecule, 6S-MGO.

Using the mono-MGO adducts of 6S or 6G that were purified from the model reaction between 6S or 6G and MGO, we studied whether 6S or 6G can inhibit the formation of AGEs through the trapping of MGO in the HSA−MGO system. 6S-MGO time-dependently formed in all the 6S-treated assays as evidenced by LC−ESI-MS (Figure 5A). Likewise, 6G-MGO was, more or less, time-dependently present in all the 6G-treated assays (Figure 5B). We demonstrated that both 6S and 6G can inhibit the formation of MGO-induced AGEs by irreversibly converting MGO into MGO adducts in the HSA−MGO system. Our results suggest that 6S and 6G may alleviate the development of diabetic complications in patients as a consequence of inhibiting MGO-induced formation of AGEs via MGO trapping.

While this study has clearly demonstrated that gingerols and shogaols could prevent the formation of AGEs via trapping of MGO, a major limitation that must be acknowledged is our results are from *in vitro* systems. The human relevance of these results needs to be proven experimentally using *in vivo* models. Trapping of MGO is a direct chemical reaction, indicating the *in vitro* findings are very likely to be confirmed *in vivo*. The MGO conjugates synthesized in this study will serve as the standards for determining the trapping of MGO by 6S and 6G in our future *in vivo* studies. However, there are many factors affecting the translation of *in vitro* findings to *in vivo*. One of these factors is the bioavailability and biotransformation of gingerols and shogaols. *In vivo* studies have shown that gingerols and shogaols are rapidly absorbed in animals and humans and accumulated in a number of tissues.[28] A pharmacokinetic study determined that the maximal concentrations of 6G, 8G, 10G, and 6S in plasma of humans were 0.85, 0.23, 0.53, and 0.15 μg/mL, respectively, after oral dosing of 2.0 g of ginger extract, which contains 43.04 mg (2.15%) of 6G, 14.40 mg (0.72%) of 8G, 33.52 mg (1.78%) of 10G, and 7.36 mg (0.37%) of 6S.[45] We recently demonstrated that both gingerols and shogaols are extensively metabolized in cancer cells, zebrafish, mice, and humans.[46−51] Whether the metabolites of gingerols and shogaols remain the trapping efficacy of MGO requires further investigation.

In conclusion, this study unveiled that both 6S and 6G could inhibit the formation of MGO-induced AGEs and consequently give rise to mono-MGO adducts, 6S-MGO and 6G-MGO, *in vitro* in the HSA−MGO system, indicating that ginger compounds, 6S and 6G, may prevent the progression of diabetic complications. Thus, consumption of ginger-containing food, beverages, or supplements, as effective and safe dietary strategies, holds great potential for preventing the development of diabetic complications and therefore enhance the quality of life and lower the morbidity and mortality of individuals with diabetes. Whether long-term intake of ginger-containing beverages or supplements to prevent or alleviate diabetic complications is effective and safe in humans is a topic for future studies.

AUTHOR INFORMATION

Corresponding Author

*Telephone: 704-250-5710. Fax: 704-250-5709. E-mail: ssang@ncat.edu or shengminsang@yahoo.com.

Funding

This paper was made possible by NPRP Grant 5-220-3-063 from the Qatar National Research Fund (a member of the Qatar Foundation).

Notes

The authors declare no competing financial interest.

ABBREVIATIONS

AGEs, advanced glycation end products; ESI, electrospray ionization; 6G, [6]-gingerol; 6G-MGO, 2-methylglyoxal [6]-gingerol; GO, glyoxal; HMBC, heteronuclear multiple-band correlation; HSA, human serum albumin; MGO, methylglyoxal; OPD, 1,2-diaminobenzene; 6S, [6]-shogaol; 6S-MGO, 2-methylglyoxal [6]-shogaol

REFERENCES

(1) Thornalley, P. J., Langborg, A., and Minhas, H. S. (1999) Formation of glyoxal, methylglyoxal and 3-deoxyglucosone in the glycation of proteins by glucose. *Biochem. J. 344*, 109−116.

(2) Guo, Q., Mori, T., Jiang, Y., Hu, C. Y., Osaki, Y., Yoneki, Y., Sun, Y., Hosoya, T., Kawamata, A., Ogawa, S., Nakayama, M., Miyata, T., and Ito, S. (2009) Methylglyoxal contributes to the development of insulin resistance and salt sensitivity in Sprague-Dawley rats. *J. Hypertens. 27*, 1664−1671.

DOI: 10.1021/acs.chemrestox.5b00293
Chem. Res. Toxicol. 2015, 28, 1842−1849

(3) Kumar, M. S., Reddy, P. Y., Kumar, P. A., Surolia, I., and Reddy, G. B. (2004) Effect of dicarbonyl-induced browning on alpha-Crystallin chaperone-like activity: physiological significance and caveats of in vitro aggregation assays. *Biochem. J. 379*, 273−282.
(4) Satish Kumar, M., Mrudula, T., Mitra, N., and Bhanuprakash Reddy, G. (2004) Enhanced degradation and decreased stability of eye lens alpha-Crystallin upon methylglyoxal modification. *Exp. Eye Res. 79*, 577−583.
(5) Baynes, J. W., Watkins, N. G., Fisher, C. I., Hull, C. J., Patrick, J. S., Ahmed, M. U., Dunn, J. A., and Thorpe, S. R. (1989) The Amadori product on protein: structure and reactions. *Prog. Clin. Biol. Res. 304*, 43−67.
(6) Bry, L., Chen, P. C., and Sacks, D. B. (2001) Effects of hemoglobin variants and chemically modified derivatives on assays for glycohemoglobin. *Clin. Chem. 47*, 153−163.
(7) Singh, R., Barden, A., Mori, T., and Beilin, L. (2001) Advanced glycation end-products: a review. *Diabetologia 44*, 129−146.
(8) Brownlee, M. (1995) Advanced protein glycosylation in diabetes and aging. *Annu. Rev. Med. 46*, 223−234.
(9) Stitt, A. W. (2001) Advanced glycation: an important pathological event in diabetic and age related ocular disease. *Br. J. Ophthalmol. 85*, 746−753.
(10) Munch, G., Shepherd, C. E., McCann, H., Brooks, W. S., Kwok, J. B., Arendt, T., Hallupp, M., Schofield, P. R., Martins, R. N., and Halliday, G. M. (2002) Intraneuronal advanced glycation endproducts in presenilin-1 Alzheimer's disease. *NeuroReport 13*, 601−604.
(11) Baynes, J. W. (2002) The Maillard hypothesis on aging: time to focus on DNA. *Ann. N. Y. Acad. Sci. 959*, 360−367.
(12) Khuhawar, M. Y., Kandhro, A. J., and Khand, F. D. (2006) Liquid chromatographic determination of glyoxal and methylglyoxal from serum of diabetic patients using meso-stilbenediamine as derivatizing reagent. *Anal. Lett. 39*, 2205−2215.
(13) Frye, E. B., Degenhardt, T. P., Thorpe, S. R., and Baynes, J. W. (1998) Role of the Maillard reaction in aging of tissue proteins. Advanced glycation end product-dependent increase in imidazolium cross-links in human lens proteins. *J. Biol. Chem. 273*, 18714−18719.
(14) Ahmed, M. U., Brinkmann Frye, E., Degenhardt, T. P., Thorpe, S. R., and Baynes, J. W. (1997) N-epsilon-(carboxyethyl)lysine, a product of the chemical modification of proteins by methylglyoxal, increases with age in human lens proteins. *Biochem. J. 324*, 565−570.
(15) Flier, J. S., Underhill, L. H., Brownlee, M., Cerami, A., and Vlassara, H. (1988) Advanced glycosylation end products in tissue and the biochemical basis of diabetic complications. *N. Engl. J. Med. 318*, 1315−1321.
(16) Kahn, S. E., Cooper, M. E., and Del Prato, S. (2014) Pathophysiology and treatment of type 2 diabetes: perspectives on the past, present, and future. *Lancet 383*, 1068−1083.
(17) Thomas, M. C., Baynes, J. W., Thorpe, S. R., and Cooper, M. E. (2005) The role of AGEs and AGE inhibitors in diabetic cardiovascular disease. *Curr. Drug Targets 6*, 453−474.
(18) Blatnik, M., Frizzell, N., Thorpe, S. R., and Baynes, J. W. (2008) Inactivation of glyceraldehyde-3-phosphate dehydrogenase by fumarate in diabetes: formation of S-(2-succinyl)cysteine, a novel chemical modification of protein and possible biomarker of mitochondrial stress. *Diabetes 57*, 41−49.
(19) Price, D. L., Rhett, P. M., Thorpe, S. R., and Baynes, J. W. (2001) Chelating activity of advanced glycation end-product inhibitors. *J. Biol. Chem. 276*, 48967−48972.
(20) Cornish, W. (2014) Safe and appropriate use of insulin and other antihyperglycemic agents in hospital. *Can. J. Diabetes 38*, 94−100.
(21) Huebschmann, A. G., Regensteiner, J. G., Vlassara, H., and Reusch, J. E. (2006) Diabetes and advanced glycoxidation end products. *Diabetes Care 29*, 1420−1432.
(22) White, B. (2007) Ginger: an overview. *Am. Fam. Physician 75*, 1689−1691.
(23) Borrelli, F., Capasso, R., Aviello, G., Pittler, M. H., and Izzo, A. A. (2005) Effectiveness and safety of ginger in the treatment of pregnancy-induced nausea and vomiting. *Obstet. Gynecol. 105*, 849−856.
(24) Portnoi, G., Chng, L. A., Karimi-Tabesh, L., Koren, G., Tan, M. P., and Einarson, A. (2003) Prospective comparative study of the safety and effectiveness of ginger for the treatment of nausea and vomiting in pregnancy. *Am. J. Obstet. Gynecol. 189*, 1374−1377.
(25) Rong, X., Peng, G., Suzuki, T., Yang, Q., Yamahara, J., and Li, Y. (2009) A 35-day gavage safety assessment of ginger in rats. *Regul. Toxicol. Pharmacol. 54*, 118−123.
(26) Chrubasik, S., Pittler, M. H., and Roufogalis, B. D. (2005) Zingiberis rhizoma: a comprehensive review on the ginger effect and efficacy profiles. *Phytomedicine 12*, 684−701.
(27) Ali, B. H., Blunden, G., Tanira, M. O., and Nemmar, A. (2008) Some phytochemical, pharmacological and toxicological properties of ginger (Zingiber officinale Roscoe): a review of recent research. *Food Chem. Toxicol. 46*, 409−420.
(28) Li, Y., Tran, V. H., Duke, C. C., and Roufogalis, B. D. (2012) Preventive and Protective Properties of Zingiber officinale (Ginger) in Diabetes Mellitus, Diabetic Complications, and Associated Lipid and Other Metabolic Disorders: A Brief Review. *Evid. Based Complement. Alternat. Med. 2012*, 516870.
(29) Saraswat, M., Reddy, P. Y., Muthenna, P., and Reddy, G. B. (2009) Prevention of non-enzymic glycation of proteins by dietary agents: prospects for alleviating diabetic complications. *Br. J. Nutr. 101*, 1714−1721.
(30) Saraswat, M., Suryanarayana, P., Reddy, P. Y., Patil, M. A., Balakrishna, N., and Reddy, G. B. (2010) Antiglycating potential of Zingiber officinalis and delay of diabetic cataract in rats. *Mol. Vision 16*, 1525−1537.
(31) Khandouzi, N., Shidfar, F., Rajab, A., Rahideh, T., Hosseini, P., and Mir Taheri, M. (2015) The effects of ginger on fasting blood sugar, hemoglobin a1c, apolipoprotein B, apolipoprotein a-I and malondialdehyde in type 2 diabetic patients. *Iran. J. Pharm. Res. 14*, 131−140.
(32) Mozaffari-Khosravi, H., Talaei, B., Jalali, B. A., Najarzadeh, A., and Mozayan, M. R. (2014) The effect of ginger powder supplementation on insulin resistance and glycemic indices in patients with type 2 diabetes: a randomized, double-blind, placebo-controlled trial. *Complement. Ther. Med. 22*, 9−16.
(33) Kubra, I. R., and Rao, L. J. (2012) An impression on current developments in the technology, chemistry, and biological activities of ginger (Zingiber officinale Roscoe). *Crit. Rev. Food Sci. Nutr. 52*, 651−688.
(34) Jolad, S. D., Lantz, R. C., Solyom, A. M., Chen, G. J., Bates, R. B., and Timmermann, B. N. (2004) Fresh organically grown ginger (Zingiber officinale): composition and effects on LPS-induced PGE2 production. *Phytochemistry 65*, 1937−1954.
(35) Sang, S., Hong, J., Wu, H., Liu, J., Yang, C. S., Pan, M. H., Badmaev, V., and Ho, C. T. (2009) Increased growth inhibitory effects on human cancer cells and anti-inflammatory potency of shogaols from Zingiber officinale relative to gingerols. *J. Agric. Food Chem. 57*, 10645−10650.
(36) Shao, X., Chen, H., Zhu, Y., Sedighi, R., Ho, C. T., and Sang, S. (2014) Essential Structural Requirements and Additive Effects for Flavonoids to Scavenge Methylglyoxal. *J. Agric. Food Chem. 62*, 3202−3210.
(37) Anguizola, J., Matsuda, R., Barnaby, O. S., Hoy, K. S., Wa, C., DeBolt, E., Koke, M., and Hage, D. S. (2013) Review: Glycation of human serum albumin. *Clin. Chim. Acta 425*, 64−76.
(38) Shaklai, N., Garlick, R. L., and Bunn, H. F. (1984) Nonenzymatic glycosylation of human serum albumin alters its conformation and function. *J. Biol. Chem. 259*, 3812−3817.
(39) Dugaiczyk, A., Law, S. W., and Dennison, O. E. (1982) Nucleotide sequence and the encoded amino acids of human serum albumin mRNA. *Proc. Natl. Acad. Sci. U. S. A. 79*, 71−75.
(40) Arasteh, A., Farahi, S., Habibi-Rezaei, M., and Moosavi-Movahedi, A. A. (2014) Glycated albumin: an overview of the In Vitro models of an In Vivo potential disease marker. *J. Diabetes Metab. Disord. 13*, 49.

DOI: 10.1021/acs.chemrestox.5b00293
Chem. Res. Toxicol. 2015, 28, 1842−1849

(41) Raghav, A., and Ahmad, J. (2014) Glycated serum albumin: a potential disease marker and an intermediate index of diabetes control. *Diabetes Metab. Syndr. 8*, 245−251.
(42) Westwood, M. E., and Thornalley, P. J. (1995) Molecular characteristics of methylglyoxal-modified bovine and human serum albumins. Comparison with glucose-derived advanced glycation endproduct-modified serum albumins. *J. Protein Chem. 14*, 359−372.
(43) Lv, L., Shao, X., Chen, H., Ho, C. T., and Sang, S. (2011) Genistein inhibits advanced glycation end product formation by trapping methylglyoxal. *Chem. Res. Toxicol. 24*, 579−586.
(44) Hu, T. Y., Liu, C. L., Chyau, C. C., and Hu, M. L. (2012) Trapping of methylglyoxal by curcumin in cell-free systems and in human umbilical vein endothelial cells. *J. Agric. Food Chem. 60*, 8190−8196.
(45) Zick, S. M., Djuric, Z., Ruffin, M. T., Litzinger, A. J., Normolle, D. P., Alrawi, S., Feng, M. R., and Brenner, D. E. (2008) Pharmacokinetics of 6-gingerol, 8-gingerol, 10-gingerol, and 6-shogaol and conjugate metabolites in healthy human subjects. *Cancer Epidemiol., Biomarkers Prev. 17*, 1930−1936.
(46) Chen, H., Soroka, D. N., Haider, J., Ferri-Lagneau, K. F., Leung, T., and Sang, S. (2013) [10]-Gingerdiols as the major metabolites of [10]-gingerol in zebrafish embryos and in humans and their hematopoietic effects in zebrafish embryos. *J. Agric. Food Chem. 61*, 5353−5360.
(47) Lv, L., Chen, H., Soroka, D., Chen, X., Leung, T., and Sang, S. (2012) 6-gingerdiols as the major metabolites of 6-gingerol in cancer cells and in mice and their cytotoxic effects on human cancer cells. *J. Agric. Food Chem. 60*, 11372−11377.
(48) Chen, H., Soroka, D., Zhu, Y., and Sang, S. (2013) Metabolism of ginger component [6]-shogaol in liver microsomes from mouse, rat, dog, monkey, and human. *Mol. Nutr. Food Res. 57*, 865−876.
(49) Chen, H., Soroka, D. N., Hu, Y., Chen, X., and Sang, S. (2013) Characterization of thiol-conjugated metabolites of ginger components shogaols in mouse and human urine and modulation of the glutathione levels in cancer cells by [6]-shogaol. *Mol. Nutr. Food Res. 57*, 447−458.
(50) Chen, H., Lv, L., Soroka, D., Warin, R. F., Parks, T. A., Hu, Y., Zhu, Y., Chen, X., and Sang, S. (2012) Metabolism of [6]-shogaol in mice and in cancer cells. *Drug Metab. Dispos. 40*, 742−753.
(51) Zhu, Y., Warin, R. F., Soroka, D. N., Chen, H., and Sang, S. (2013) Metabolites of ginger component [6]-shogaol remain bioactive in cancer cells and have low toxicity in normal cells: chemical synthesis and biological evaluation. *PLoS One 8*, e54677.

DOI: 10.1021/acs.chemrestox.5b00293
Chem. Res. Toxicol. 2015, 28, 1842−1849